ACCSCIENCE PUBLISHING

Eurasian Journal of Medicine and Oncology

ORIGINAL RESEARCH ARTICLE

Fluorine-18 fluorodeoxyglucose positron emission tomography/computed tomography metabolic characteristics in nasopharyngeal carcinoma with synchronous versus metachronous distant metastasis

Rong Huang, Yan Tang, and Yun Zhang*

Department of PET/CT Center, Jiangsu Cancer Hospital, Jiangsu Institute of Cancer Research, The Affiliated Cancer Hospital of Nanjing Medical University, Nanjing, Jiangsu, China

Abstract

Introduction: Prior studies seldom accounted for the timing of distant metastasis (DM) when linking tumor metabolism to metastatic potential. To fill this key research gap, this study investigates the metabolic heterogeneity among three DM subgroups: non-DM, metachronous DM (MDM), and synchronous DM (SDM).

Objectives: To explore the metabolic characteristics of DM-stratified nasopharyngeal carcinoma (NPC) cohorts.

Methods: This retrospective study included 281 patients with NPC who underwent pre-treatment fluorine-18 fluorodeoxyglucose positron emission tomography/computed tomography. Metabolic parameters of the primary tumor (PT) and metastatic lymph node (MLN) were compared across three groups. Parameters associated with MDM and SDM were analyzed statistically.

Results: Demographic and clinical characteristics were comparable among groups (all $p > 0.05$). All PT and MLN metabolic parameters differed significantly across groups (all $p < 0.05$): PT parameters were higher in SDM/MDM than in non-DM ($p < 0.05$) without SDM–MDM differences, whereas MLN parameters increased sequentially with significant pairwise comparisons (all $p < 0.05$). Univariate regression revealed stronger associations between MLN parameters and MDM and SDM. Binary logistic regression identified distinct independent correlates: MDM was positively associated with PT glucose-normalized total lesion glycolysis and MLN glucose-normalized maximum standardized uptake value (SUVmax), and negatively with MLN mean SUV; SDM showed only positive correlates, including PT metabolic tumor volume, MLN metabolic tumor volume, and MLN lean body mass-normalized SUVmax.

Conclusion: This study systematically characterized metabolic heterogeneity across DM trajectories (non-DM, MDM, SDM). MLN metabolic parameters were more sensitive and robust than PT parameters, with distinct independent correlates for MDM and SDM.

Keywords: Nasopharyngeal carcinoma; Fluorine-18 fluorodeoxyglucose positron emission tomography/computed tomography; Metabolic heterogeneity; Metachronous distant metastasis; Synchronous distant metastasis

***Corresponding author:**
Yun Zhang
(zhangchunyandu@163.com)

Citation: Huang R, Tang Y, Zhang Y. Fluorine-18 fluorodeoxyglucose positron emission tomography/computed tomography metabolic characteristics in nasopharyngeal carcinoma with synchronous versus metachronous distant metastasis. *Eurasian J Med Oncol.* doi: 10.36922/EJMO026080092

Received: February 22, 2026

Revised: May 21, 2026

Accepted: May 25, 2026

Published online: June 24, 2026

Copyright: © 2026 Author(s). This is an Open-Access article distributed under the terms of the Creative Commons Attribution License, permitting distribution, and reproduction in any medium, provided the original work is properly cited.

Publisher's Note: AccScience Publishing remains neutral with regard to jurisdictional claims in published maps and institutional affiliations.

1. Introduction

Nasopharyngeal carcinoma (NPC) is a type of head and neck cancer arising from the nasopharyngeal epithelium[1]. NPC development is associated with genetic susceptibility, Epstein–Barr virus infection, and environmental factors such as smoking.[2] NPC is highly prevalent in endemic regions worldwide. Approximately 120,000 new cases occur worldwide annually, with nearly 80% across South, East, and Southeast Asia, contrasting sharply with the rarity of the disease in Western populations.[3] Projections indicate that global NPC incidence and mortality will increase substantially by 2040, with a pronounced increase in Asian populations.[4] With the widespread use of radiotherapy and chemotherapy, NPC-related mortality has declined, and the five-year survival rate has improved overall. Local recurrence and distant metastasis (DM) remain the primary challenges in NPC treatment and major contributors to patient mortality.[5]

Nasopharyngeal carcinoma DM is classified as synchronous distant metastases (SDM) and metachronous distant metastases (MDM). SDM is defined as DM detected at the time of initial NPC diagnosis or within three months after completion of definitive radiotherapy. MDM is defined as DM detected more than three months after completion of definitive radiotherapy.[6] In the clinical management of NPC, fluorine-18 fluorodeoxyglucose positron emission tomography/computed tomography (^{18}F-FDG PET/CT) provides high diagnostic accuracy with a low false-positive rate for detecting cervical lymph nodes and DM. Accordingly, leading authoritative oncology guideline organizations recommend it as a key imaging modality for clinical management.[7] Patients initially staged with PET/CT showed better long-term disease control than those without PET/CT staging.[8] Aerobic glycolysis, an emerging hallmark of NPC, contributes to immune evasion, tumor growth, and proliferation.[9] As a widely utilized metabolic imaging modality in nuclear medicine, ^{18}F-FDG PET/CT rapidly captures heterogeneity in glucose metabolism between tumor and normal cells.[10] ^{18}F-FDG PET/CT parameters offer valuable metabolic insights for clinical decision-making in oncology, and are well established for assessing tumor aggressiveness[11] and lymph node metastasis (LNM)[11], evaluating treatment response[12], guiding personalized therapy[13,14], and forecasting patient survival outcomes.[15,16] Overall, these findings suggest that metabolic parameters can be used to assess metabolic heterogeneity in NPC. Apart from the extensively applied maximum standardized uptake value (SUVmax), numerous volumetric parameters and normalized indices have been developed to overcome the drawbacks of single-point uptake metrics, thereby comprehensively characterizing tumor metabolism. These include metabolic tumor volume (MTV), total lesion glycolysis (TLG)[17], lean body mass-normalized SUVmax (SULmax)[18,19], body surface area-normalized SUVmax (SUSmax)[20], and glucose-normalized SUVmax/SUVmean/TLG (GNmax, GNmean, GNTLG).[21,22]

However, a critical research gap persists in the current understanding of NPC metabolic characteristics: while ^{18}F-FDG PET/CT parameters have been validated for evaluating general tumor metabolic activity and assessing metastatic risk, existing studies have not systematically explored metabolic heterogeneity between the primary tumor (PT) and the most metabolically active metastatic lymph nodes (MLN) across patients stratified by the timing of DM (i.e., SDM, MDM, and no metastasis within five years). Notably, SDM and MDM differ substantially in clinical presentation, treatment strategies, and prognostic outcomes, implying potential differences in underlying metabolic mechanisms. Yet few studies have specifically examined whether the metabolic profiles of PT and MLN vary among these three clinically distinct subgroups, nor have they identified subgroup-specific metabolic parameters that correlate with SDM or MDM. This oversight limits the translation of metabolic imaging findings into targeted risk stratification and personalized management for NPC patients with different metastatic patterns.

Therefore, this study aims to explore whether metabolic heterogeneity exists between the PT and the most metabolically active MLN across three groups of patients with NPC: those with SDM, those with MDM, and those without metastasis within five years after treatment. Additionally, this study aims to investigate the association between PET/CT metabolic parameters and SDM and MDM.

2. Materials and methods

2.1. Study design

This was a single-center retrospective study focusing on DM in NPC patients, including non-DM, SDM and MDM. The study collected clinical, imaging, and follow-up data of eligible NPC patients, and analyzed the metabolic parameters of PT and MLN derived from ^{18}F-FDG PET/CT to explore their correlation with metastatic status.

2.1.1. Participants

Patients with NPC who underwent ^{18}F-FDG PET/CT at Jiangsu Cancer Hospital between May 2017 and October 2024 were retrospectively reviewed. This study enrolled eligible participants according to predefined inclusion and

exclusion criteria. The patient selection process is detailed in Figure 1.

Inclusion criteria included patients (i) aged ≥ 18 years; (ii) with histopathologically confirmed squamous cell carcinoma via endoscopic biopsy; (iii) who underwent neck magnetic resonance imaging (MRI) prior to any treatment; (iv) with clinical staging according to the 9th TNM classification[23]; and (v) who were able to complete standardized follow-up as required.

Exclusion criteria included (i) patients with incomplete visualization of the nasopharyngeal lesion on PET images (e.g., due to motion artifacts, inadequate field of view, or severe image noise); and (ii) those with a history of other malignant tumors.

A total of 1,750 patients were initially screened. After

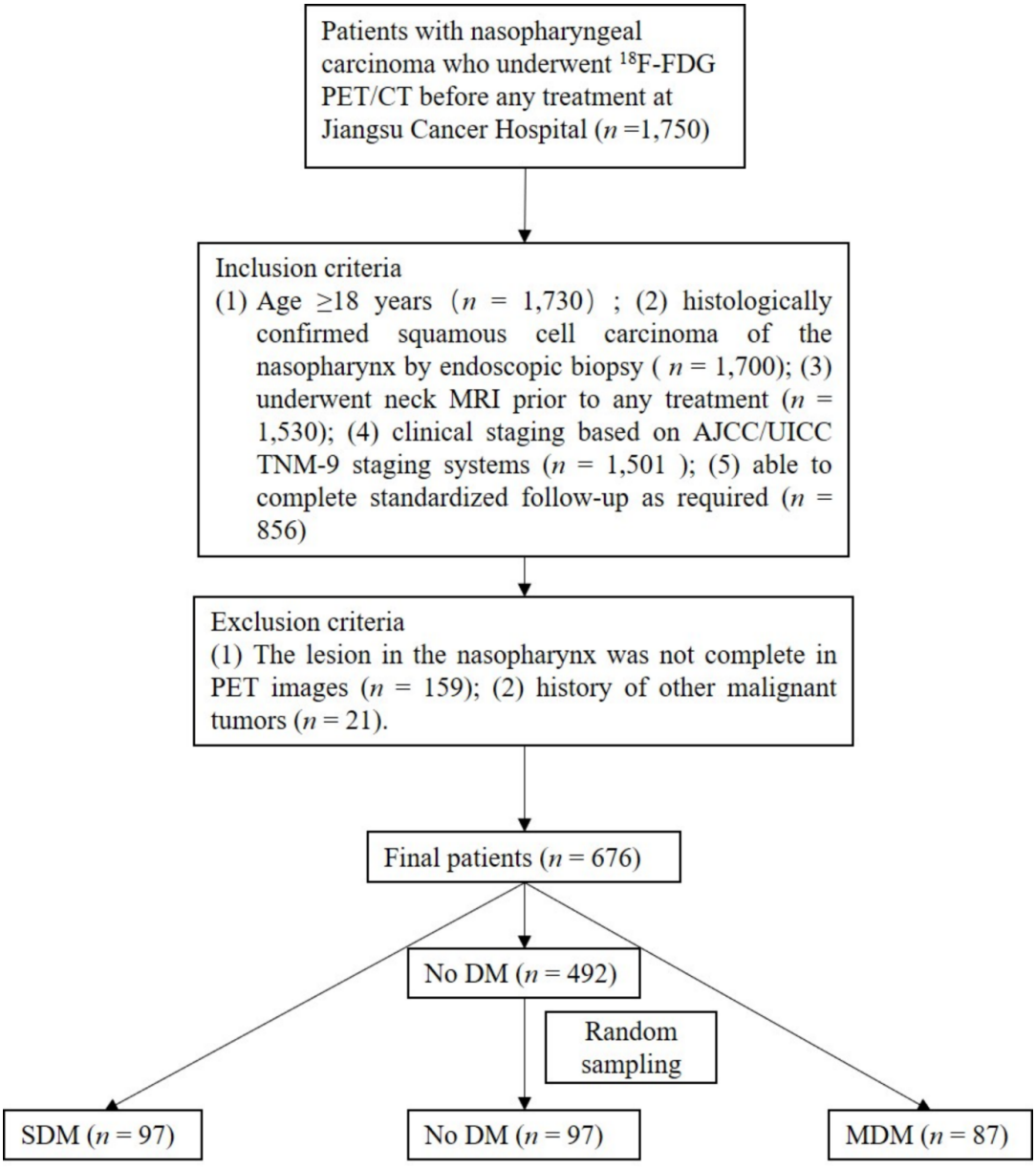


Figure 1. Flowchart of patient selection
Abbreviations: DM: Distant metastasis; 18F-FDG PET/CT: Fluorine-18 fluorodeoxyglucose positron emission tomography/computed tomography; MDM: Metachronous distant metastasis; MRI: Magnetic resonance imaging; SDM: Synchronous distant metastasis.

applying inclusion and exclusion criteria, 676 eligible patients were identified. Of these, 97 had SDM, 87 had MDM, and 492 were non-DM. To ensure balanced group sizes, 97 patients were randomly selected from the non-DM group, resulting in a final cohort of 281 patients (97 SDM, 87 MDM, 97 non-DM).

2.1.2. Follow-up strategy

The follow-up started after definitive radiotherapy and ended on October 31, 2024, or at DM occurrence, loss to follow-up, or death (whichever came first). The follow-up frequency was once every three months in the first two years, once every six months in the 3rd–5th years, and once yearly after five years. Follow-up methods included outpatient review, telephone follow-up, and online messaging follow-up. Follow-up contents included symptom inquiry, physical examination, tumor marker detection, and imaging examinations (cervical MRI every six months, ^{18}F-FDG PET/CT, or CT every 12 months or when suspected DM occurred). All suspected DM lesions were confirmed by pathological biopsy or ≥2 imaging examinations to ensure diagnostic accuracy. Patients lost to follow-up were recorded in detail, and follow-up data were verified by designated personnel. Notably, the actual follow-up duration before MDM classification varied among patients who developed MDM, reflecting differences in the timing of metastasis.

2.1.3. Definition and verification of synchronous distant metastasis and metachronous distant metastasis

Synchronous DM is defined as DM diagnosed at initial NPC presentation or within three months after definitive radiotherapy completion. All SDM cases were confirmed by pathological biopsy or at least two independent imaging examinations (PET/CT, CT, or MRI) with an interval of more than four weeks. Lesions with non-progressive inflammatory or radiation-induced FDG elevation were strictly excluded to avoid false diagnosis of DM. MDM is defined as DM diagnosed more than three months after completion of definitive radiotherapy.

Consistent with the above confirmation criteria for SDM, all metastatic lesions (including SDM and MDM) were confirmed at the initial clinical presentation (by pathological biopsy or imaging demonstrating typical metastatic features) or during post-treatment follow-up. For lesions lacking immediate confirmation, patients underwent intensive imaging surveillance (PET/CT, CT, or MRI) every three months for at least 12 months. Progressively enlarging lesions were classified as DM, whereas stable or regressive lesions were reclassified as benign or locoregional, ensuring diagnostic accuracy and reliability.

Non-DM patients were defined as those with no DM within five years post-treatment, who were strictly confirmed through the standardized follow-up protocol and randomly selected from 500 NPC patients without DM during the same study period. Simple random sampling was used for selection, without stratification or manual selection, effectively eliminating selection bias and ensuring an unbiased sample. The sample size of 97 was chosen to match the SDM group (n = 97), ensuring balanced sample distribution across the three study groups (non-DM = 97, MDM = 87, SDM = 97). A balanced sample size between groups improves the stability of intergroup comparative analysis and statistical robustness. Meanwhile, the baseline demographic and clinical characteristics of the three groups were well balanced (all $p > 0.05$), which further verifies the rationality and representativeness of the randomly selected control group.

2.1.4. Positron emission tomography/computed tomography imaging protocol

All patients underwent ^{18}F-FDG PET/CT scanning on a Discovery 710 system (GE Medical Systems, United States). Prior to radiotracer administration, patients fasted for at least six h, and blood glucose levels below 11 mmol/L were confirmed to meet imaging criteria. ^{18}F-FDG (0.1–0.2 mCi/kg) was administered intravenously. After a 50–70 min uptake phase, during which patients drank 1,000 mL of water and voided immediately before scanning, images were acquired from the vertex to the mid-thigh.

Imaging parameters were set as follows:

(i) CT: 140 kV tube voltage; automatic milliampere (mA); 0.8-s rotation time; 3.75-mm slice thickness.
(ii) PET: 2 min per bed position across 6–7 bed positions.
(iii) Reconstruction: Iterative reconstruction with CT attenuation correction was performed using the VUE point FX + SharpIR algorithm (2 iterations, 24 subsets).

All images were postprocessed and analyzed on an AW 4.6 workstation (GE Healthcare, United States).

2.1.5. Image interpretation and volume of interest delineation

Two radiologists with over 10 years of clinical experience independently interpreted the images, remaining blinded to the patients' metastatic status and clinical follow-up data. Volumes of interest (VOIs) were delineated on the PT and the most metabolically active MLN according to a previously validated methodology.[24] All generated VOIs were subsequently reviewed and manually

corrected on a slice-by-slice basis to ensure accuracy and to avoid interference from surrounding normal tissues. Interobserver agreement for metabolic parameter measurement was assessed using the intraclass correlation coefficient; values > 0.75 indicated good agreement, and any discrepancies were resolved by consensus.

2.1.6. Metabolic parameter definitions and extraction

Metabolic parameters for the PT and the most FDG-avid MLN were derived using a fixed 42% SUVmax threshold.[25] The definitions of each metabolic parameter are as follows:

(i) SUVmax/SUVmean: Maximum and mean SUVs were within the defined VOI[21]. SUVmax refers to the highest uptake value of ^{18}F-FDG in the VOI of PT or MLN, which directly reflects the most metabolically active area of the tumor and is an important indicator of tumor cell proliferation activity. SUVmean is the average of all SUV values in the VOI, which makes up for the limitation of SUVmax that only reflects local maximum metabolic activity, and comprehensively reflects the overall metabolic level of the entire tumor tissue, helping to evaluate the homogeneity of tumor metabolism.

(ii) Peak SUV (SUVpeak): Mean SUV within a small, fixed-size VOI encompassing the area of highest radiotracer uptake.[26] Unlike SUVmax, which uses only the voxel with the highest uptake, SUVpeak calculates the average uptake within a small, fixed-volume region around that voxel. This parameter has higher measurement stability and reproducibility, which can effectively reduce measurement error due to individual differences in VOI delineation by radiologists, and is more suitable for inter-group comparisons of metabolic parameters in multi-case studies.

(iii) SULmax: SUVmax normalized to the lean body mass.[27] Since SUVmax is affected by the patient's total body weight, especially body fat content, there may be significant differences in SUVmax values between patients with different body types even if their tumor metabolic activity is similar. SULmax corrects SUVmax for lean body mass, eliminating interference from body fat and weight differences and making the metabolic parameters of PT and MLN more comparable across patients in this study.

(iv) SUSmax: SUVmax normalized to body surface area.[28] Similar to SULmax, SUSmax is a normalized parameter of SUVmax, which uses body surface area (calculated based on the patient's height and weight) for correction. This correction method is particularly suitable for patients with extreme body weight (too light or too heavy), thereby ensuring comparability of metabolic parameters across the study population and improving the scientific rigor of intergroup analysis.

(v) GNmax/GNmean: Glucose-normalized SUVmax and SUVmean, respectively.[21,22] As a glucose analog, ^{18}F-FDG's uptake by tumor cells is directly affected by the patient's blood glucose level before imaging—elevated blood glucose will compete with ^{18}F-FDG for uptake by tumor cells, leading to falsely decreased SUV values. GNmax and GNmean correct SUVmax and SUVmean by the patient's fasting blood glucose level (measured before radiotracer injection), eliminating the interference of blood glucose fluctuations, and ensuring the accuracy of metabolic parameter measurement in all enrolled patients (**Equation 1**).

$$\text{GNmax/GNmean} = \text{SUVmax/SUVmean} \times (\text{blood glucose level [mmol/L]/ 5.56}) \quad (1)$$

(vi) MTV: Total tumor volume comprising voxels exceeding the 42% SUVmax threshold.[25] MTV reflects the actual volume of tumor tissue with abnormally high metabolic activity in PT and MLN, which differs from the anatomical tumor volume measured by CT or MRI. It not only reflects the size of the tumor but also is closely related to the number of metabolically active tumor cells, which is an important indicator of tumor load. In this study, MTV was used to evaluate the total volume of malignant lesions in PT and MLN.

(vii) TLG: Product of MTV and SUVmean.[25] TLG combines two core indicators of tumor metabolism (SUVmean, reflecting overall metabolic activity) and tumor load (MTV, reflecting the volume of metabolically active tissue), comprehensively quantifying the total glycolytic activity of the entire tumor. Compared with a single parameter (SUVmax, MTV, or SUVmean), TLG more accurately reflects the overall malignant potential of PT and MLN.

(viii) GNTLG: Product of MTV and GNmean.[21,22] On the basis of TLG, GNTLG further uses blood glucose level for correction (through GNmean), eliminating the interference of blood glucose fluctuations on the quantification of total tumor glycolytic activity. This parameter integrates the advantages of glucose correction and comprehensive metabolic load evaluation.

(ix) NTR: MLNSUVmax/PTSUVmax.[29] NTR is the ratio of SUVmax of the most metabolically active MLN to SUVmax of the PT, which is used to evaluate the relative metabolic activity between MLN and PT. This parameter can reflect the metabolic heterogeneity between the PT and its MLN, and explore whether

the metabolic activity of the MLN is consistent with that of the PT, providing a reference for analyzing the metastasis mechanism and biological characteristics of NPC.

2.2. Study setting

This study was conducted at our tertiary-care Grade A center. Clinical, imaging and follow-up data of NPC patients were retrospectively collected from May 2017 to October 2024. All patients underwent standardized ^{18}F-FDG PET/CT imaging prior to initial anti-tumor treatment with dedicated equipment and unified protocols. This retrospective study was approved by the Ethics Committee of Jiangsu Cancer Hospital on December 12, 2024, with informed consent waived for data de-identification.

2.3. Statistical analysis

2.3.1. Data preprocessing and normality/variance homogeneity tests

Prior to formal statistical analysis, all metabolic parameters (PT and hypermetabolic lymph node indices) were assessed for missing data. For parameters with <5% missingness, complete case analysis was used; no significant missing data were observed for key parameters in this study. The normality of metabolic parameter distributions was assessed using the Shapiro–Wilk test. The homogeneity of variance for each metabolic parameter across all three groups was evaluated using Levene's test.

2.3.2. Intergroup comparison of metabolic parameters

One-way analysis of variance was applied to normally distributed parameters with equal variance to compare PT and MLN parameters across the three groups. Bonferroni-corrected post-hoc tests were conducted for pairwise comparisons when overall significance was observed ($p < 0.05$).

The Kruskal–Wallis H test was applied to parameters that violated the assumptions of normality or homogeneity of variance. Bonferroni-corrected Dunn's test was used for pairwise comparisons when the overall effect was significant ($p < 0.05$).

2.3.3. Correlation analysis

Binary logistic regression was performed for two-group comparisons (Non-DM vs. MDM; Non-DM vs. SDM), using metabolic parameters (PT and MLN indices) as independent variables and group status as the dependent variable. Odds ratios (OR) and 95% confidence intervals (CIs) were calculated to quantify the strength of the correlation. All univariate logistic regression p-values were Bonferroni-corrected ($\alpha = 0.05/21 \approx 0.0024$) before variable selection for multivariable models to reduce type I error and ensure statistical robustness.

Spearman's rank correlation analysis was applied when bivariate normality was not satisfied to evaluate monotonic relationships between PT and MLN metabolic parameters, with statistical significance determined by p-values.

2.3.4. Statistical software and significance level

All statistical analyses were performed using the Statistical Package for Social Sciences 22.0 software (IBM Corp., United States). Two-tailed p-values < 0.05 were considered statistically significant. Multiple comparisons were corrected (e.g., Bonferroni) to control type I error. To ensure the reliability of the subgroup regression analysis, the sample size and statistical power were assessed: in line with the requirements of multivariate logistic regression, each subgroup has at least 10 events per independent variable. In both MDM and SDM multivariate models, only three key parameters were included. Combined with McFadden's R^2 values (0.159 for MDM and 0.306 for SDM), the sample size of 281 patients was sufficient to ensure the stability and reliability of subgroup regression analysis.

3. Results

3.1. Demographic and clinical characteristics

Table 1 summarizes the demographic and clinical data for the three patient cohorts (non-DM, MDM, and SDM). Regarding demographic characteristics, no significant differences were observed among the three groups in age, sex distribution, blood glucose levels, height, or weight (all $p > 0.05$). This baseline homogeneity is clinically significant, as it indicates that differences in DM status among the three groups are not attributable to individual baseline characteristics, thereby excluding potential confounding factors and ensuring the reliability of subsequent analyses of metabolic parameters. In addition, the mean blood glucose levels of the three groups were all below 11 mmol/L, meeting the requirements of PET/CT imaging and ensuring the accuracy of metabolic parameter measurement. All patients in the present cohort had complete and standardized fasting blood glucose data before ^{18}F-FDG injection, with a documented fasting blood glucose data availability rate of 100%. This ensures the accurate calculation and reliable application of glucose-normalized metabolic parameters (GNmax, GNmean, GNTLG) in our correlation analysis. For tumor T/N staging, the SDM group had a higher proportion of advanced stages: the T4 stage proportion was 53.6% (52/97), 24.7% higher than that of the non-DM group (28.9%, 28/97), suggesting that PT invasion depth is closely

Table 1. Demographic and clinical characteristics of patients

Parameter	Non-DM (n = 97)	MDM (n = 87)	SDM (n = 97)	H/χ^2	p
Age (years), mean ± SD	49.56 ± 12.50	51.44 ± 12.68	52.87 ± 12.04	1.738	0.178
Sex (M/F)	68/29	66/21	80/17	4.079	0.130
Blood glucose (mmol/L), mean ± SD	5.69 ± 0.97	5.95 ± 1.04	5.77 ± 0.97	1.546	0.215
Height (cm), mean ± SD	168.32 ± 7.78	167.41 ± 6.96	167.30 ± 7.81	0.526	0.592
Weight (kg), mean ± SD	66.81±11.30	67.29±11.61	66.30±12.54	0.162	0.850
T1	13 (13.4%)	6 (6.9%)	5 (5.2%)		
T2	24 (24.7%)	11 (12.6%)	14 (14.4%)		
T3	32 (33.0%)	34 (39.1%)	26 (26.8%)		
T4	28 (28.9%)	36 (41.4%)	52 (53.6%)		
N0	9 (9.3%)	2 (2.3%)	0		
N1	52 (53.6%)	30 (34.5%)	20 (20.6%)		
N2	30 (30.9%)	36 (41.4%)	33 (34.0%)		
N3	6 (6.2%)	19 (21.8%)	44 (45.4%)		
M1a	0	0	42 (43.3%)		
M1b	0	0	55 (56.7%)		

Note: * $p < 0.05$. Data presented as n (%), unless stated otherwise.
Abbreviations: DM: Distant metastasis; MDM: Metachronous distant metastasis; SDM: Synchronous distant metastasis.

related to synchronous DM. The N3 stage proportion in the SDM group was 45.4% (44/97), significantly higher than in the non-DM group (6.2%, 6/97) and the MDM group (21.8%, 19/87), indicating that the extent of lymph node metastasis is positively correlated with DM risk.

3.2. Comparison of metabolic parameters of primary tumors and high-metabolic activity lymph nodes

Table 2 summarizes the metabolic parameter comparison of the PT and MLN among the three groups. Overall, all metabolic parameters (SUV-related indices, glucose-normalized parameters, volume-based parameters, normalized SUV values, and R) differed significantly among groups (all $p < 0.05$), indicating that PT and MLN metabolic characteristics are closely related to NPC DM and can effectively distinguish patients with different metastasis risks.

Pairwise comparison results (Table 3, Figures 2 and 3) showed that the SDM and MDM groups had significantly higher values than the non-DM group for all PT metabolic parameters (all $p < 0.05$), with no significant differences between the SDM and MDM groups (all $p > 0.05$). This may be because the metabolic activity of PT in both metastasis groups is at a high threshold, weakening its ability to distinguish metastasis timing. In contrast, MLN metabolic parameters increased progressively from the non-DM to the MDM and SDM groups, with all pairwise

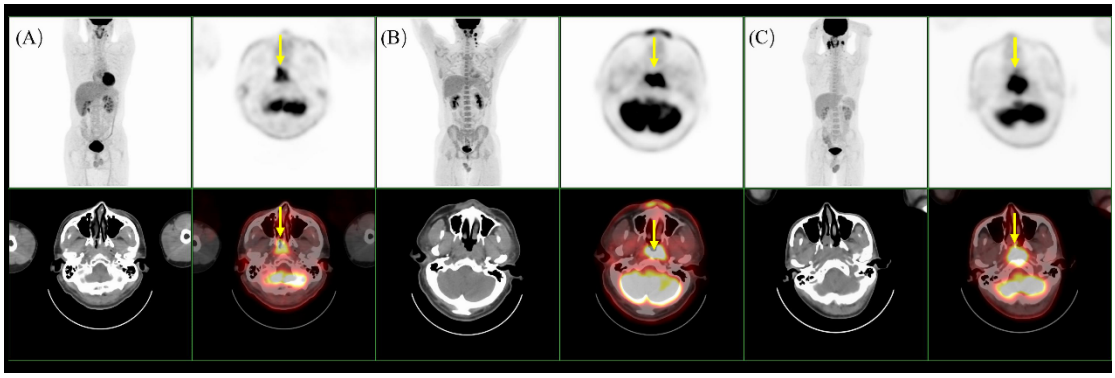


Figure 2. ^{18}F-FDG PET–CT imaging of primary tumors (yellow arrows) in patients with (A) non-DM, (B) MDM, and (C) SDM nasopharyngeal carcinoma, respectively
Abbreviations: DM: Distant metastasis; ^{18}F-FDG PET/CT: Fluorine-18 fluorodeoxyglucose positron emission tomography/computed tomography; MDM: Metachronous distant metastasis; SDM: Synchronous distant metastasis.

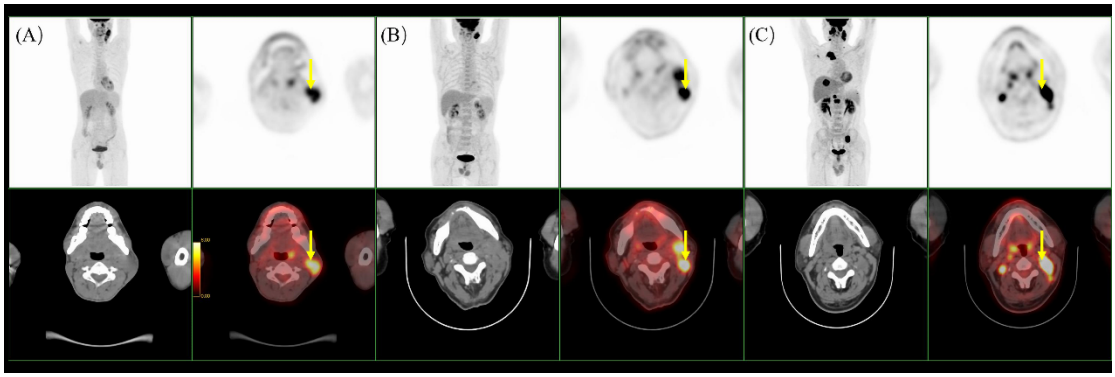


Figure 3. ^{18}F-FDG PET–CT imaging of metastatic lymph nodes (yellow arrows) in patients with (A) non-DM, (B) MDM, and (C) SDM nasopharyngeal carcinoma, respectively
Abbreviations: DM: Distant metastasis; ^{18}F-FDG PET/CT: Fluorine-18 fluorodeoxyglucose positron emission tomography/computed tomography; MDM: Metachronous distant metastasis; SDM: Synchronous distant metastasis.

comparisons significant (all $p < 0.05$), indicating that MLN metabolic characteristics can distinguish both the presence and timing of metastasis. NTR was significantly lower in the non-DM group than in the MDM and SDM groups ($p = 0.042$ and $p = 0.004$, respectively), with no difference between the MDM and SDM groups ($p = 0.415$), suggesting that the NTR is related to the occurrence of metastasis but not to its timing.

3.3. Univariate logistic regression analysis

Univariate logistic regression was performed to assess the association between metabolic parameters and the risk of MDM and SDM (Table 4). For MDM, most PT and MLN metabolic parameters were significant risk factors ($p < 0.0024$), except for NTR ($p = 0.062$), MLNMTV ($p = 0.069$), MLNTLG ($p = 0.016$) and MLNGNTLG ($p = 0.010$). For SDM, most PT and MLN metabolic parameters were significant risk factors ($p < 0.0024$), except for NTR ($p = 0.003$), with particularly high ORs for MLNSUSmax (OR = 2.022, 95% CI: 1.587–2.576), PTSUSmax (OR = 1.505, 95% CI: 1.218 –1.860), and R (OR = 2.279, 95% CI: 1.324–3.922). Overall, MLN-related metabolic parameters showed stronger associations with MDM and SDM risk than PT-related parameters, as indicated by higher ORs.

3.4. Correlation analysis between primary tumor and high-metabolic activity lymph node metabolic parameters

Spearman's rank correlation analysis was performed to assess the relationship between PT and MLN metabolic

Table 2. Comparison of metabolic parameters of primary tumors and lymph nodes with the highest activity among three groups

Parameter	Non-DM (*n* = 97)	MDM (*n* = 87)	SDM (*n* = 97)	*F*/H	*p*
PTSUVmax	11.90 ± 5.04	14.02 ± 5.43	15.32 ± 6.15	9.322	0.000**
PTSUVmean	7.25 ± 3.25	8.54 ± 3.25	9.27 ± 3.78	8.556	0.000**
PTGNmax	11.81 ± 5.16	14.38 ± 5.68	15.22 ± 6.42	9.064	0.000**
PTGNmean	7.20 ± 3.31	8.75 ± 3.37	9.20 ± 3.92	8.458	0.000**
PTSUVpeak	9.14 ± 4.32	10.95 ± 4.40	12.22 ± 5.17	10.730	0.000**
PTSULmax	9.43 ± 4.07	11.12 ± 4.27	12.24 ± 4.96	9.813	0.000**
PTSUSmax	3.17 ± 1.39	3.71 ± 1.47	4.10 ± 1.72	8.914	0.000**
MLNSUVmax	8.39 ± 5.33	12.24 ± 5.44	14.76 ± 6.04	31.587	0.000**
MLNSUVmean	5.32 ± 3.35	7.63 ± 3.50	9.25 ± 3.99	28.765	0.000**
MLNGNmax	8.37 ± 5.35	12.63 ± 5.76	14.67 ± 6.32	29.510	0.000**
MLNGNmean	5.30 ± 3.35	7.91 ± 3.70	9.19 ± 4.15	27.161	0.000**
MLNSUVpeak	6.46 ± 4.11	9.30 ± 4.68	11.19 ± 4.92	24.949	0.000**
MLNSULmax	6.59 ± 4.29	9.64 ± 4.24	11.73 ± 4.63	33.649	0.000**
MLNSUSmax	2.30 ± 1.61	3.21 ± 1.40	3.90 ± 1.57	26.607	0.000**
NTR	0.82 ± 0.60	1.00 ± 0.69	1.07 ± 0.54	4.576	0.011*
PTMTV (mL)	6.130 (3.5, 9.5)	6.520 (4.1, 13.8)	9.870 (5.1, 17.4)	14.734	0.001**
PTTLG (g)	36.530 (19.0, 70.5)	62.660 (29.2, 147.9)	85.750 (48.6, 167.3)	25.212	0.000**
PTGNTLG (g)	37.570 (19.6, 69.6)	64.050 (30.3, 145.1)	84.140 (46.6, 162.6)	24.006	0.000**
MLNMTV (mL)	2.260 (1.0, 5.4)	3.520 (2.0, 5.7)	4.870 (2.0, 8.9)	19.950	0.000**
MLNTLG (g)	10.720 (4.3, 35.3)	29.630 (10.6, 47.7)	38.440 (17.2, 86.3)	35.834	0.000**
MLNGNTLG (g)	10.860 (4.4, 32.4)	32.520 (10.6, 52.4)	36.830 (15.4, 84.8)	36.133	0.000**

Note: * $p < 0.05$, ** $p < 0.01$.

Abbreviations: DM: Distant metastasis; GN: Glucose normalized; MDM: Metachronous distant metastasis; MLN: Metastatic lymph node; MTV: Mean tumor volume; NTR: Node-to-tumor ratio; PT: Primary tumor; SDM: Synchronous distant metastasis; SUL: Lean body mass-normalized SUV; SUS: Body surface area-normalized SUV; SUV: Standardized uptake value; TLG: Total lesion glycolysis.

Table 3. Pairwise comparison results among three groups

Parameter	(I) group	(J) group	(I) median/mean	(J) median/mean	Difference (I–J)	*p*
PTSUVmax	Non-DM	MDM	11.899	14.023	−2.124	0.010*
	Non-DM	SDM	11.899	15.317	−3.418	0.000**
	MDM	SDM	14.023	15.317	−1.294	0.116
PTSUVmean	Non-DM	MDM	7.251	8.540	−1.289	0.012*
	Non-DM	SDM	7.251	9.271	−2.020	0.000**
	MDM	SDM	8.540	9.271	−0.731	0.151
PTGNmax	Non-DM	MDM	11.815	14.377	−2.562	0.003**
	Non-DM	SDM	11.815	15.216	−3.401	0.000**
	MDM	SDM	14.377	15.216	−0.839	0.327

(*Cont'd...*)

Table 3. (***Continued***)

Parameter	(I) group	(J) group	(I) median/mean	(J) median/mean	Difference (I–J)	*p*
	Non-DM	MDM	7.196	8.749	−1.553	0.003**
PTGNmean	Non-DM	SDM	7.196	9.201	−2.005	0.000**
	MDM	SDM	8.749	9.201	−0.452	0.389
	Non-DM	MDM	9.138	10.951	−1.813	0.009**
PTSUVpeak	Non-DM	SDM	9.138	12.219	−3.082	0.000**
	MDM	SDM	10.951	12.219	−1.269	0.066
	Non-DM	MDM	9.427	11.117	−1.691	0.011*
PTSULmax	Non-DM	SDM	9.427	12.243	−2.816	0.000**
	MDM	SDM	11.117	12.243	−1.125	0.088
	Non-DM	MDM	3.171	3.715	−0.543	0.017*
PTSUSmax	Non-DM	SDM	3.171	4.097	−0.926	0.000**
	MDM	SDM	3.715	4.097	−0.383	0.092
	Non-DM	MDM	8.391	12.243	−3.852	0.000**
MLNSUVmax	Non-DM	SDM	8.391	14.762	−6.371	0.000**
	MDM	SDM	12.243	14.762	−2.519	0.003**
	Non-DM	MDM	5.324	7.632	−2.308	0.000**
MLNSUVmean	Non-DM	SDM	5.324	9.254	−3.931	0.000**
	MDM	SDM	7.632	9.254	−1.623	0.003**
	Non-DM	MDM	8.368	12.630	−4.262	0.000**
MLNGNmax	Non-DM	SDM	8.368	14.673	−6.306	0.000**
	MDM	SDM	12.630	14.673	−2.044	0.018*
	Non-DM	MDM	5.297	7.909	−2.612	0.000**
MLNGNmean	Non-DM	SDM	5.297	9.194	−3.897	0.000**
	MDM	SDM	7.909	9.194	−1.285	0.021*
	Non-DM	MDM	6.463	9.302	−2.839	0.000**
MLNSUVpeak	Non-DM	SDM	6.463	11.189	−4.727	0.000**
	MDM	SDM	9.302	11.189	−1.888	0.006**
	Non-DM	MDM	6.585	9.645	−3.060	0.000**
MLNSULmax	Non-DM	SDM	6.585	11.733	−5.148	0.000**
	MDM	SDM	9.645	11.733	−2.088	0.001**
	Non-DM	MDM	2.300	3.212	−0.911	0.000**
MLNSUSmax	Non-DM	SDM	2.300	3.902	−1.601	0.000**
	MDM	SDM	3.212	3.902	−0.690	0.003**
	Non-DM	MDM	0.815	1.000	−0.184	0.042*
NTR	Non-DM	SDM	0.815	1.073	−0.258	0.004**
	MDM	SDM	1.000	1.073	−0.074	0.415

(*Cont'd...*)

Table 3. (*Continued*)

Parameter	(I) group	(J) group	(I) median/mean	(J) median/mean	Difference (I–J)	*p*
	Non-DM	MDM	6.130	6.520	−0.390	0.031*
PTMTV (mL)	Non-DM	SDM	6.130	9.870	−3.740	0.000**
	MDM	SDM	6.520	9.870	−3.350	0.119
	Non-DM	MDM	36.530	62.660	−26.130	0.002**
PTTLG (g)	Non-DM	SDM	36.530	85.750	−49.220	0.000**
	MDM	SDM	62.660	85.750	−23.090	0.077
	Non-DM	MDM	37.570	64.050	−26.480	0.001**
PTGNTLG (g)	Non-DM	SDM	37.570	84.140	−46.570	0.000**
	MDM	SDM	64.050	84.140	−20.090	0.146
	Non-DM	MDM	2.260	3.520	−1.260	0.005**
MLNMTV (mL)	Non-DM	SDM	2.260	4.870	−2.610	0.000**
	MDM	SDM	3.520	4.870	−1.350	0.145
	Non-DM	MDM	10.720	29.630	−18.910	0.000**
MLNTLG (g)	Non-DM	SDM	10.720	38.440	−27.720	0.000**
	MDM	SDM	29.630	38.440	−8.810	0.022*
	Non-DM	MDM	10.860	32.520	−21.660	0.000**
MLNGNTLG (g)	Non-DM	SDM	10.860	36.830	−25.970	0.000**
	MDM	SDM	32.520	36.830	−4.310	0.045*

Note: * $p < 0.05$, ** $p < 0.01$.

Abbreviations: DM: Distant metastasis; GN: Glucose normalized; MDM: Metachronous distant metastasis; MLN: Metastatic lymph node; MTV: Mean tumor volume; NTR: Node-to-tumor ratio; PT: Primary tumor; SDM: Synchronous distant metastasis; SUL: Lean body mass-normalized SUV; SUS: Body surface area-normalized SUV; SUV: Standardized uptake value; TLG: Total lesion glycolysis.

parameters (Table 5). Except for MLNMTV, which showed no correlation with any PT parameters (all $p > 0.05$), most MLN metabolic parameters showed low-to-moderate monotonic association with most PT metabolic parameters (excluding PT metabolic tumor volume [PTMTV]), with correlation coefficients of 0.121–0.330 (all $p < 0.05$), suggesting PT and MLN metabolic characteristics have certain consistency (derived from the same tumor cells) and independence (affected by different microenvironments). Among these, the strongest correlations were between PTSUVpeak and MLNSUVpeak ($r = 0.330$, $p < 0.01$) and between PTGNmean and MLNGNmean ($r = 0.324$, $p < 0.01$), reflecting high consistency in peak metabolic activity and glucose-corrected average metabolic activity between PT and MLN.

3.5. Binary logistic regression analysis of the association between positron emission tomography parameters and synchronous distant metastasis and metachronous distant metastasis

Binary logistic regression analysis was performed to identify independent PET metabolic parameters associated with MDM and SDM; model fit was assessed by McFadden R^2 (Tables 6 and 7). For correlation with MDM, the final model revealed three significant parameters: PTGNTLG (regression coefficient = 0.006, $p = 0.006$, OR = 1.006, 95% CI: 1.002–1.010) and MLN glucose-normalized maximum SUV (MLNGNmax; regression coefficient = 0.460, $p = 0.004$, OR = 1.584, 95% CI: 1.163–2.158) as positive correlates, and MLN mean SUV (MLNSUVmean) (regression coefficient = −0.547, $p = 0.030$, OR = 0.578, 95% CI: 0.353–0.949) as a negative correlate. The McFadden R^2 of this model was 0.159, indicating a moderate fit and that these three parameters explain 15.9% of the variation in MDM. For correlation with SDM, three parameters were significant independent positive correlates: PTMTV (regression coefficient = 0.110, $p = 0.001$, OR = 1.116, 95% CI: 1.056–1.180), MLNMTV (regression coefficient = 0.072, $p = 0.030$, OR = 1.074, 95% CI: 1.007–1.146), and MLN lean body mass-normalized SUVmax (MLNSULmax, regression coefficient = 0.244, $p = 0.001$, OR = 1.276, 95% CI: 1.164–1.399). McFadden R^2 for the SDM correlation model was 0.306, indicating a moderate fit and that these three parameters explain 30.6% of SDM variation.

Table 4. Univariate logistic regression analysis results

Variables	MDM		SDM	
	p	OR (95% CI)	*p*	OR (95% CI)
PTSUVmax	0.008	1.083 (1.021–1.149)	0.000	1.120 (1.058–1.186)
PTSUVmean	0.010	1.132 (1.030–1.243)	0.000	1.183 (1.082–1.294)
PTGNmax	0.003	1.095 (1.032–1.161)	0.000	1.110 (1.051–1.172)
PTGNmean	0.003	1.153 (1.050–1.266)	0.000	1.170 (1.073–1.275)
PTSUVpeak	0.007	1.102 (1.027–1.182)	0.000	1.151 (1.076–1.232)
PTSULmax	0.008	1.104 (1.026–1.188)	0.000	1.505 (1.077–1.244)
PTSUSmax	0.013	1.315 (1.059–1.634)	0.000	1.505 (1.218–1.860)
MLNSUVmax	0.000	1.142 (1.076–1.213)	0.000	1.231 (1.151–1.316)
MLNSUVmean	0.000	1.221 (1.111–1.342)	0.000	1.371 (1.234–1.522)
MLNGNmax	0.000	1.149 (1.083–1.220)	0.000	1.213 (1.139–1.293)
MLNGNmean	0.000	1.238 (1.127–1.360)	0.000	1.345 (1.217–1.486)
MLNSUVpeak	0.000	1.162 (1.078–1.253)	0.000	1.505 (1.171–1.379)
MLNSULmax	0.000	1.183 (1.097–1.276)	0.000	1.305 (1.199–1.421)
MLNSUSmax	0.000	1.521 (1.221–1.894)	0.000	2.022 (1.587–2.576)
NTR	0.062	1.582 (0.978–2.560)	0.003	2.279 (1.324 –3.922)
PTMTV	0.006	1.055 (1.016–1.096)	0.000	1.088 (1.041–1.137)
PTTLG	0.002	1.006 (1.002–1.010)	0.000	1.009 (1.005–1.014)
PTGNTLG	0.001	1.007 (1.003–1.011)	0.000	1.009 (1.005–1.014)
MLNMTV	0.069	1.079 (0.994–1.171)	0.001	1.129 (1.051–1.213)
MLNTLG	0.016	1.011 (1.002–1.019)	0.000	1.017 (1.008–1.026)
MLNGNTLG	0.010	1.012 (1.003–1.020)	0.000	1.017 (1.008–1.026)

Note: $p < 0.0024$.

Abbreviations: CI: Confidence interval; DM: Distant metastasis; GN: Glucose normalized; MDM: Metachronous distant metastasis; MLN: Metastatic lymph node; MTV: Mean tumor volume; NTR: Node-to-tumor ratio; OR: Odds ratio; PT: Primary tumor; SDM: Synchronous distant metastasis; SUL: Lean body mass-normalized SUV; SUS: Body surface area-normalized SUV; SUV: Standardized uptake value; TLG: Total lesion glycolysis.

Table 5. Correlation coefficients between metabolic parameters of primary tumors and those of lymph nodes with the highest activity

Parameter	PTMTV	PTSUVmax	PTSUVmean	PTTLG	PTGNmax	PTGNmean	PTSUSmax	PTSULmax	PTGNTLG	PTSUVpeak
MLNMTV	−0.073	0.032	0.016	−0.028	0.026	0.016	0.010	0.028	−0.024	0.044
MLNSUVmax	0.044	0.309**	0.294**	0.171**	0.289**	0.276**	0.262**	0.301**	0.167**	0.316**
MLNSUVmean	0.051	0.319**	0.304**	0.181**	0.295**	0.282**	0.276**	0.315**	0.175**	0.327**
MLNTLG	−0.040	0.144*	0.128*	0.043	0.130*	0.119*	0.110	0.138*	0.042	0.154**
MLNGNmax	0.067	0.282**	0.265**	0.179**	0.324**	0.310**	0.231**	0.270**	0.203**	0.291**
MLNGNmean	0.076	0.296**	0.280**	0.193**	0.337**	0.324**	0.248**	0.286**	0.216**	0.306**
MLNGNTLG	−0.027	0.138*	0.121*	0.053	0.158**	0.146*	0.102	0.131*	0.069	0.149*
MLNSUVpeak	0.036	0.325**	0.311**	0.171**	0.302**	0.291**	0.279**	0.316**	0.167**	0.330**
MLNSULmax	0.051	0.317**	0.302**	0.180**	0.289**	0.276**	0.280**	0.324**	0.173**	0.325**
MLNSUSmax	0.052	0.307**	0.293**	0.180**	0.280**	0.268**	0.291**	0.312**	0.172**	0.316**

Note: * $p < 0.05$, ** $p < 0.01$.

Abbreviations: DM: Distant metastasis; GN: Glucose normalized; MDM: Metachronous distant metastasis; MLN: Metastatic lymph node; MTV: Mean tumor volume; NTR: Node-to-tumor ratio; PT: Primary tumor; SDM: Synchronous distant metastasis; SUL: Lean body mass-normalized SUV; SUS: Body surface area-normalized SUV; SUV: Standardized uptake value; TLG: Total lesion glycolysis.

doi: 10.36922/EJMO026080092

Table 6. Association of positron emission tomography parameters with metachronous distant metastasis

Variables	Regression coefficient	Standard error	*z*	Wald χ^2	*p*	OR	95% CI
PTGNTLG	0.006	0.002	2.767	7.654	0.006	1.006	1.002–1.010
MLNSUVmean	−0.547	0.252	−2.168	4.702	0.030	0.578	0.353–0.949
MLNGNmax	0.460	0.158	2.919	8.520	0.004	1.584	1.163–2.158
Intercept	−1.839	0.392	−4.691	22.007	0.000	0.159	0.074–0.343

Note: Dependent variable = group; McFadden $R^2 = 0.159$.
Abbreviations: CI: Confidence interval; GN: Glucose normalized; MLN: Metastatic lymph node; OR: Odds ratio; PT: Primary tumor; SUV: Standardized uptake value; TLG: Total lesion glycolysis.

Table 7. Association of positron emission tomography parameters with synchronous distant metastasis

Variables	Regression coefficient	Standard error	*z*	Wald χ^2	*p*	OR	95% CI
PTMTV	0.110	0.028	3.910	15.285	0.000	1.116	1.056–1.180
MLNMTV	0.072	0.033	2.165	4.689	0.030	1.074	1.007–1.146
MLNSULmax	0.244	0.047	5.206	27.101	0.000	1.276	1.164–1.399
Intercept	−3.706	0.576	−6.437	41.441	0.000	0.025	0.008–0.076

Note: Dependent variable = group; McFadden $R^2 = 0.306$.
Abbreviations: MLN: Metastatic lymph node; MTV: Mean tumor volume; PT: Primary tumor; SUL: Lean body mass-normalized SUV; SUV: Standardized uptake value.

4. Discussion

4.1. Study innovation and research gap addressment

To our knowledge, this is the first study to examine metabolic heterogeneity across three patient cohorts stratified by DM status: non-DM, MDM, and SDM. This novel stratification fills an important research gap, since most prior works only described correlations between tumor metabolic activity and metastatic risk, while neglecting the timing of DM. This study identifies prognostic associations, not causal drivers, of DM timing in NPC patients.

4.2. Metabolic heterogeneity across distant metastasis cohorts: Primary tumor vs. metastatic lymph node discriminatory ability

Primary tumor and MLN metabolic activities were the highest in the SDM group, intermediate in the MDM group, and lowest in the non-DM group. This stepwise metabolic gradient across the three subgroups parallels the varying metastatic phenotypes and may correlate with distinct biological profiles related to tumor aggressiveness and metastatic propensity.

First, SDM tumors exhibit intrinsic molecular characteristics that correlate with metabolic reprogramming and early distant dissemination. Elevated glucose uptake in SDM is closely linked to enhanced glycolysis (the Warburg effect), a metabolic phenotype that correlates with abundant energy and biosynthetic intermediates as well as aggressive tumor behaviors including proliferation, invasion and distant progression[9]. Key regulators of this process, including hexokinase 2, lactate dehydrogenase A, phosphofructokinase 1, and pyruvate kinase M2, are frequently upregulated in highly metastatic tumors, and their upregulation correlates with enhanced glucose uptake and lactate accumulation in metastatic phenotypes.[9,30,31]

Notably, our results showed distinct differences in the discriminatory performance between PT and MLN metabolic parameters. All PT metabolic indices were significantly elevated in the SDM and MDM groups compared with the non-DM group, with no statistically significant difference between the SDM and MDM subgroups. This finding may reflect a plateau effect in PT metabolism. Metabolic levels of the PT were elevated in both metastatic subgroups, which is associated with a limited capacity to distinguish DM patterns. In contrast, MLN metabolic parameters showed a progressive increase from the non-DM group to the MDM group and further to the SDM group, with significant differences in all pairwise comparisons. This gradient change is closely associated with the clinical characteristics of different metastatic trajectories: SDM is characterized by DM at initial diagnosis, which is associated with the strongest intrinsic invasiveness of the tumor, while MDM occurs after primary treatment, which is associated with moderate metastatic potential, and non-DM tumors have the lowest invasiveness. In this context, MLN metabolic features not only differentiate patients with or without DM but also correlate with varying degrees of metastatic aggressiveness and chronological patterns of distant failure. These observations support the putative role of lymph nodes as a metastatic hub in NPC.

4.3. Metabolic phenotypes and metastatic potential: Correlation between primary tumor/metastatic lymph node metabolism and distant metastasis

Metachronous DM is characterized by intermediate metabolic features that are associated with a unique pretreatment tumor phenotype. Tumors in this subgroup display moderate metastatic activity between the non-DM and SDM groups, and pre-treatment metabolic indices correlate with the occurrence of delayed DM. In contrast, tumors in the non-DM group present lower metabolic profiles, alongside less aggressive biological phenotypes.

Our data demonstrate distinct tumor metabolic heterogeneity across the three cohorts. This gradient trend was especially pronounced in MLN-related parameters, with significant differences observed in all pairwise comparisons among the three groups. Metabolic heterogeneity is more prominent in MLNs than in PTs, and lymph node metabolic status is strongly associated with systemic metastatic susceptibility.

This finding is further supported by our correlation analysis, which showed low-to-moderate monotonic associations between most PT and MLN metabolic parameters (correlation coefficients ranging from 0.121 to 0.330, all $p < 0.05$), except for MLNMTV, which showed no correlation with any PT parameters. This dual pattern of consistency and independence may be linked to the biological origin and distinct microenvironments of PT and MLN. On one hand, MLN tumor cells originate from the primary lesion and exhibit partial metabolic similarities to PT cells. On the other hand, PT and MLN reside in distinct tissue microenvironments; for instance, MLN is characterized by an immunosuppressive niche that differs from that of PT. Such microenvironmental divergence may correlate with distinct metabolic alterations in lymph nodes, and these metabolic differences are associated with the superior discriminatory efficacy of MLN metabolic parameters for metastatic profiles.

4.4. Stronger correlation of metastatic lymph node metabolic parameters for metastatic status

Metastatic lymph node metabolic parameters increased sequentially across the three groups. Longitudinal metabolic features of lymph nodes are correlated with DM and may act as a potential marker for metastatic risk. These observations are consistent with the primary finding that MLN metabolic indices show stronger correlations with metastatic status than PT indicators do. Binary logistic regression results further illustrated this trend: MLN-derived markers (e.g., MLNGNmax for MDM, OR = 1.584; MLNSULmax for SDM, OR = 1.276) presented higher odds ratios compared with PT-related parameters (e.g., PTGNTLG for MDM, OR = 1.006; PTMTV for SDM, OR = 1.116).

Several previous studies have identified PT characteristics and cervical MLN status as key correlates of SDM[32,33], and advanced N stage has been recognized as an independent risk factor.[32] Consistent with these findings, our data indicated that MLN metabolic indices showed stronger correlations with SDM than with PT parameters. Such metabolic differences may be associated with improved risk stratification.

4.5. Study advantages

Most existing studies concerning NPC metabolism and DM merely differentiate patients with or without SDM. In comparison, the present study adopted a novel grouping strategy based on DM timing (non-DM, MDM and SDM), and systematically analyzed metabolic alterations in both PTs and MLN. This stratified design allows for a more refined evaluation of distinct metastatic patterns and provides comprehensive metabolic profiling, which may complement the limitations of previous research regarding DM timingrelated metabolic correlations.

4.6. Discrepancies with existing studies and metabolic parameter correlation profiles

Although metabolic parameters are widely used to assess MDM[15,16,29,34], their application in SDM assessment remains limited. Additionally, studies reported NTR as a correlate of MDM[29,34], but our study showed no association between NTR and MDM. This discrepancy may be related to the differences in study design: existing studies mostly did not stratify patients by DM timing, and the sample composition and tumor subtypes may also differ from our study; more importantly, our study focused on the correlation between NTR and MDM, rather than its predictive value, which may also be associated with differences in the interpretation of results.

Multiple metabolic parameters were correlated with MDM and SDM, and obvious intercorrelations existed among these indicators. Binary logistic regression identified PTGNTLG and MLNGNmax as positive correlates, and MLNSUVmean as a negative correlate for MDM, whereas PTMTV, MLNMTV, and MLNSULmax were relevant indicators for SDM. Distinct correlation patterns were observed between the two metastatic subgroups: MDM exhibited correlations with both positive and negative metabolic markers, while only positive metabolic correlates were identified in the SDM cohort.

Notably, our study identified MLN SUVmean as an independent negative correlate of MDM (OR = 0.578). This counterintuitive finding challenges the conventional view that higher metabolic activity uniformly correlates with greater tumor aggressiveness, and it may be partially explained by potential links to intratumoral metabolic heterogeneity, metabolic symbiosis, and immune–metabolic crosstalk within MLN.

First, a lower MLN SUVmean may reflect increased intratumoral metabolic heterogeneity rather than diminished malignant potential. As demonstrated by Pellegrino *et al.*[35], the coefficient of variation of FDG uptake is an established index of glycolytic heterogeneity. This parameter is independently correlated with favorable survival in patients with advanced non-small cell lung cancer. In contrast, a low coefficient of variation, indicating homogeneous high FDG uptake, tends to coincide with poor prognosis. In MLN, a reduced SUVmean does not necessarily indicate uniformly inactive metabolism; instead, it may reflect spatially mixed metabolic subclones, including hypoxic or necrotic areas with low FDG uptake interspersed with highly glycolytic regions. This heterogeneous distribution is accompanied by lower overall SUVmean and appears to coincide with a structurally complex tumor ecosystem potentially related to subsequent distant dissemination.

Second, this inverse association shows potential relevance to the lactate-driven metabolic symbiosis model (reverse Warburg effect) in MLN, as comprehensively reviewed by Cruz and Barba.[36] Under physiological oxygen and nutrient gradients in MLN, tumor cells may display a complementary lactate shuttle pattern, in which hypoxic tumor subclones show vigorous aerobic glycolysis with abundant lactate production and lactate extrusion via MCT4, while adjacent normoxic tumor cells tend to take up extracellular lactate through MCT1 and preferentially utilize lactate for oxidative phosphorylation, which is linked to decreased glucose consumption and FDG uptake. This spatially coordinated metabolic pattern correlates with a reduced overall SUVmean and is potentially related to improved energy utilization, altered nutrient-

stress response, and sustained tumor cell invasiveness and survival phenotypes. Importantly, such metabolic symbiosis patterns are likely linked to metastatic potential rather than indolent tumor behavior.

Third, immune–metabolic crosstalk further facilitates the interpretation of this paradoxical correlation. Lee *et al.*[37] reported that in colorectal cancer, low metabolic heterogeneity (uniform FDG uptake) correlates with increased CD163+ M2 macrophage infiltration, elevated interleukin-6 levels, and worse recurrence-free survival. By extension, MLN with lower SUVmean and greater metabolic heterogeneity may be associated with relatively preserved anti-tumor immune activity at baseline. However, lactate accumulation within the symbiotic microenvironment shows potential links to altered immune status, which may correlate with suppressed CD8+ T cell function, shifted M2 macrophage polarization tendency, elevated programmed death-ligand 1 expression, and altered immune evasion profiles.[36] Over time, these interconnected metabolic and immune features coincide with increased likelihood of silent systemic seeding, which may be associated with the higher observed MDM risk among cases with lower MLN SUVmean.

In summary, the negative correlation between MLN SUVmean and MDM risk is potentially linked to adaptive metabolic symbiosis patterns and elevated intratumoral metabolic heterogeneity. These two biological features coincide with altered metastatic potential alongside reduced global glucose uptake. These findings emphasize that SUVmean alone is insufficient to stratify metastatic risk; incorporating metabolic heterogeneity and immune–metabolic profiles may help improve MDM risk assessment and refine risk stratification for patients with MLN.

4.7. Value of glucose-normalized parameters in metachronous distant metastasis correlation

Glucose-normalized parameters (PTGNTLG, MLNGNmax) emerged as key correlates for MDM, despite their limited clinical application and uncertain value in diagnostic evaluation and treatment monitoring.[21] This limitation is closely associated with the inherent properties of ^{18}F-FDG. As a glucose analog, ^{18}F-FDG competes with endogenous glucose for the same membrane transporters. Under hyperglycemic conditions, such competitive interactions are associated with decreased tracer uptake and altered biodistribution in tumor tissues.[38,39]

To address this, the European Association of Nuclear Medicine procedure guidelines recommend that patients fast prior to FDG PET/CT imaging to achieve stable blood glucose levels; in cases of hyperglycemia, hypoglycemic agents should be administered to reduce blood glucose to a target level below 200 mg/dL, and no glucose correction of SUV values is required when blood glucose remains under this threshold.[21] Currently, no evidence demonstrates that GN and GNTLG improve treatment response monitoring or outcome assessment compared to uncorrected SUV. A recent study has reported that the efficacy of glucose correction remains inconsistent across tumor types, and its performance may be affected by SUV metrics, normalization strategies, and imaging platforms. Appropriate selection of normalization approaches is thus closely correlated with rigorous clinical practice, and SUVmean appears to exhibit better stability and reproducibility after glucose normalization.[22]

Despite these clinical limitations, glucose-normalized parameters are correlated with attenuated confounding effects of blood glucose fluctuations and favorable metabolic profiling. The present findings provide additional insights into the metabolic correlates of MDM in NPC patients, particularly among those with abnormal glucose levels.

4.8. Comparison of metachronous distant metastasis and synchronous distant metastasis correlation model fit

Furthermore, the SDM correlation model showed a better fit than the MDM model, with McFadden R^2 values of 0.306 and 0.159, respectively. The metabolic markers screened for SDM (PTMTV, MLNMTV, MLNSULmax) exhibited more stable correlations, suggesting distinct metabolic phenotypes across metastatic subgroups. Within the SDM-related signature, volume-based indices (PTMTV, MLNMTV) quantify the overall burden of metabolically active lesions. By contrast, MLNSULmax minimizes the confounding effects of body weight and adipose tissue, showing stable correlational performance with SDM.

This study focuses on exploratory associations between metabolic parameters and metastatic patterns (SDM, MDM, no-DM) rather than establishing formal clinical predictive models. Thus, discrimination metrics (e.g., area under the curve, calibration plots) were not provided, as our binary logistic regression analyses aimed to identify independent correlates rather than validate predictive efficacy. Prospective validation with receiver operating characteristic analysis and external multi-center cohort testing would be required for clinical translation of the findings, to confirm the utility of key metabolic parameters in routine metastatic risk stratification.

4.9. Research significance

Overall, the present study systematically characterized metabolic heterogeneity in PTs and MLN across NPC

patients with distinct DM patterns, and assessed the associations between metabolic indices and DM onset as well as its temporal features. These observations provide additional insights into the biological profiles of different metastatic subtypes and expand current evidence regarding metabolic signatures and DM in NPC. Consistent with the research objectives, this analysis further illustrates distinct metabolic distribution patterns correlated with NPC metastasis. Such findings may be conducive to clinical understanding of variable metastatic phenotypes, especially in regions with a high NPC prevalence.

4.10. Limitations of the study

Despite the novel findings and clinical implications of this study, several limitations should be acknowledged to ensure a comprehensive interpretation of the results and provide guidance for future research. First, the cross-sectional design only captures PT and MLN metabolic characteristics at a single pre-therapy time point, failing to establish a causal relationship between metabolic activity and DM timing or track dynamic metabolic changes during tumor progression. Thus, we cannot confirm whether observed metabolic heterogeneity is a cause or consequence of different metastatic trajectories. Second, the molecular mechanisms underlying metabolic heterogeneity were not validated at the tissue level. Our inference linking enhanced SDM glucose metabolism to the Warburg effect lacks direct molecular evidence (e.g., immunohistochemistry, RNA sequencing), restricting comprehensive interpretation of the association between MLN metabolic features and metastatic status. Third, the single-center design with a relatively small sample size may limit result generalizability and the robustness of binary logistic regression models, even with moderate model fit (McFadden R^2 = 0.159 for MDM, 0.306 for SDM). Fourth, potential confounding factors (tumor differentiation, treatment regimens, follow-up duration) were not accounted for, which may interfere with the association between pre-therapy metabolic parameters and metastatic status. Fifth, although we strictly confirmed SDM cases by pathological biopsy or at least two independent imaging examinations with an interval of more than four weeks and excluded lesions with non-progressive inflammatory or radiation-induced FDG elevation, there remains a potential risk of false positives due to the difficulty in completely distinguishing radiation-induced uptake from true metastatic lesions, which may be correlated with minor fluctuations in the diagnostic accuracy of SDM identification. Sixth, given the limitations of the current research design (the primary purpose was to explore the association and metabolic heterogeneity between PET metabolic parameters and metastatic patterns, rather than to establish and validate a clinical prediction model), we did not perform receiver operating characteristic and area under the curve comparison analysis between GNmax and uncorrected SUVmax for MDM prediction. The predictive models should be verified, and the efficacy of glucose-normalized parameters should be quantified in future independent cohorts.

Moreover, although a standardized 42% SUVmax threshold was adopted for VOI delineation, volumetric metabolic indices (including MTV and TLG) are sensitive to segmentation methods and threshold selection. We further clarify that while the absolute values of MTV and TLG should be interpreted cautiously, the relative group comparisons conducted in this study (e.g., pairwise comparisons of MLNMTV across non-DM, MDM, and SDM groups) remain valid and statistically reliable, as all analyses used the same standardized segmentation protocol to ensure consistency. Additionally, this study primarily focused on exploring the associations between PET metabolic indices and metastatic patterns, with no relevant assessment of demographic and clinical covariates such as age, sex, T stage, N stage, and fasting blood glucose. Correspondingly, these clinical variables were not included in the univariate screening or multivariate regression modeling. The primary purpose of this design was to centralize the research focus on tumor metabolic features and reduce unnecessary confounding factors. Notably, baseline clinical and demographic characteristics were well balanced among the non-DM, MDM, and SDM groups (all $p > 0.05$), which could largely mitigate the potential confounding effects of these variables on metabolic correlation analyses. Further largesample studies with comprehensive adjustment for clinical covariates are warranted to validate and extend our current findings.

4.11. Future research directions

Based on the study's limitations and novel findings, future research should address existing gaps, deepen understanding of the association between tumor metabolic heterogeneity and DM, and promote clinical translation. First, prospective longitudinal studies with larger samples are needed to track dynamic PT/MLN metabolic changes, clarify their association with metastatic timing, and identify more sensitive dynamic metabolic indicators. Second, combining PET imaging with molecular profiling (e.g., immunohistochemistry, RNA sequencing) will further characterize metabolic heterogeneity and clarify the stronger association of MLN metabolic parameters with metastatic status relative to PT parameters. Third, multicenter studies with diverse cohorts will validate metabolic profiles, improve result generalizability, and optimize regression models by expanding the sample

size. Fourth, incorporating confounding factors (tumor differentiation, treatment regimens, etc.) into analyses will refine the understanding of the association between metabolic parameters and metastatic status. Fifth, clinical validation studies should evaluate the practical value of key metabolic parameters (e.g., MLNGNmax for MDM; PTMTV, MLNMTV, MLNSULmax for SDM) and glucose-normalized parameters in routine practice. Finally, extending findings to other tumor types will explore whether the association between MLN metabolic parameters and DM is universal, expanding the study's clinical significance.

5. Conclusion

Our study systematically characterized metabolic heterogeneity across patients with distinct DM trajectories (non-DM, MDM, SDM). The data indicate that MLN-related metabolic parameters exhibit stronger correlations than PT indices. Differential independent metabolic markers were further identified for MDM and SDM, with unique correlation patterns observed in each subgroup. These findings provide novel supplemental evidence for metastatic risk stratification and individualized clinical management in NPC, and highlight the potential prognostic relevance of MLN.

Acknowledgments

None.

Funding

This study received funding from the special project of clinical research on truth-seeking by Jiangsu Cancer Hospital under grant number ZL202210.

Conflict of interest

The authors declare they have no competing interests.

Author contributions

Conceptualization: Yun Zhang
Data curation: All authors
Formal analysis: Yun Zhang, Rong Huang
Investigation: Yun Zhang
Methodology: Yun Zhang
Writing–original draft: Yun Zhang, Rong Huang
Writing–review & editing: Yun Zhang

Ethics approval and consent to participate

This retrospective multicenter study was approved by the Institutional Ethics Review Boards of Jiangsu Cancer Hospital (protocol code ky-2024-132; approval date: December 12, 2024). The requirement for informed consent was waived because of the retrospective nature of the study.

Consent for publication

Not applicable. The requirement for informed consent was waived because of the retrospective nature of the study.

Availability of data

The datasets used and/or analyzed during the current study are available from the corresponding author on reasonable request.

References

1. Cantu G. Nasopharyngeal carcinoma. A "different" head and neck tumour. Part B: treatment, prognostic factors, and outcomes. *Acta Otorhinolaryngol Ital*. 2023;43(3):155-169.

   doi: 10.14639/0392-100X-N2223

2. Su ZY, Siak PY, Lwin YY, *et al.* Epidemiology of nasopharyngeal carcinoma: current insights and future outlook. *Cancer Metastasis Rev*. 2024;43(3):919-939.

   doi: 10.1007/s10555-024-10176-9

3. Ferlay J, Ervik M, Lam F, *et al.* Global Cancer Observatory: Cancer Today. Lyon: International Agency for Research on Cancer; 2024. Accessed Mar 10, 2025. https://gco.iarc.fr/today

4. Zhang Y, Gu S, Deng H, *et al.* Global epidemiological profile in nasopharyngeal carcinoma: a prediction study. *BMJ Open*. 2024;14(12):e091087.

   doi: 10.1136/bmjopen-2024-091087

5. Qu W, Li S, Zhang M, *et al.* Pattern and prognosis of distant metastases in nasopharyngeal carcinoma: A large-population retrospective analysis. *Cancer Med*. 2020;9(17):6147-6158.

   doi: 10.1002/cam4.3301

6. Pan CC, Lu J, Chen P, *et al.* 1016 Li biyan'ai yuanchu zhuanyi huanzhe de zhuanyi cenceng xihua jiqi linchuang yiyi [Evaluation of the prognostic significance of refinement and stratification of distant metastasis status in 1016 cases of nasopharyngeal carcinoma]. *Chin J Oncol*. 2013;35(8):595-599. [In Chinese]

   doi: 10.3760/cma.j.issn.0253-3766.2013.08.007

7. Colevas AD, Yom SS, Pfister DG, *et al.* NCCN Guidelines Insights: Head and Neck Cancers, Version 1. 2018. *J Natl Compr Canc Netw*. 2018;16(5):479-490.

   doi: 10.6004/jnccn.2018.0026

8. Niu X, Xue F, Ou D, *et al.* Pretreatment FDG PET in prognosis of locoregionally advanced nasopharyngeal carcinoma treated with intensity-modulated radiation therapy. *Int J Med Sci*. 2025;22(4):933-939.

   doi: 10.7150/ijms.105995

9. Pan Z, Liu Y, Li H, *et al.* The role and mechanism of aerobic glycolysis in nasopharyngeal carcinoma. *PeerJ*. 2025;13:e19213.

doi: 10.7717/peerj.19213

10. Shangguan C, Gan G, Zhang J, *et al.* Cancer-associated fibroblasts enhance tumor (18)F-FDG uptake and contribute to the intratumor heterogeneity of PET-CT. *Theranostics*. 2018;8(5):1376-1388.

doi: 10.7150/thno.22717

11. Zhang Y, Hu Y, Zhao S, *et al.* The Utility of (18)F-FDG-PET-CT Metabolic Parameters in Evaluating the Primary Tumor Aggressiveness and Lymph Node Metastasis of Nasopharyngeal Carcinoma. *Clin Med Insights Oncol*. 2024;18:11795549231225419.

doi: 10.1177/11795549231225419

12. Quartuccio N, Sireci F, Pulizzi S, *et al.* Predictive Value of [(18)F]FDG PET/CT for Neoadjuvant Chemoradiotherapy Response in Nasopharyngeal Carcinoma. *J Clin Med*. 2025;14(18);6508.

doi: 10.3390/jcm14186508

13. Fu XB, Li TT, Fei ZD, *et al.* Role of PET/CT in improving the cost effectiveness of nimotuzumab in nasopharyngeal carcinoma. *Acta Otorhinolaryngol Ital*. 2024;44(5):296-305.

doi: 10.14639/0392-100X-N2827

14. Qiu HZ, Zhang X, Liu SL, *et al.* M1 stage subdivisions based on (18)F-FDG PET-CT parameters to identify locoregional radiotherapy for metastatic nasopharyngeal carcinoma. *Ther Adv Med Oncol*. 2022;14:17588359221118785.

doi: 10.1177/17588359221118785

15. John C, Venkatasai J, Kondaveeti SS, *et al.* Prognostic significance of metabolic tumour volume and maximum standard uptake value of fluor-18-fluorodeoxyglucose positron emission tomography with computed tomography in nasopharyngeal carcinoma. *Contemp Oncol*. 2021;25(3):153-159.

doi: 10.5114/wo.2021.109620

16. Dongxiang W, Liting L, Yujing L, *et al.* Prediction of outcomes in patients with local recurrent nasopharyngeal carcinoma: development and validation of a four-factor prognostic model integrating baseline characteristics and [(18)F]FDG PET/CT parameters. *Eur Radiol*. 2022;33(4):2840-2849.

doi: 10.1007/s00330-022-09232-1

17. Larson SM, Erdi Y, Akhurst T, *et al.* Tumor Treatment Response Based on Visual and Quantitative Changes in Global Tumor Glycolysis Using PET-FDG Imaging. *Clinical Positron Imaging*. 1999;2(3):159-171.

doi: 10.1016/S1095-0397(99)00016-3

18. Sarikaya I, Albatineh AN, Sarikaya A. Revisiting Weight-Normalized SUV and Lean-Body-Mass-Normalized SUV in PET Studies. *J Nucl Med Technol*. 2020;48(2):163-167.

doi: 10.2967/jnmt.119.233353

19. Samim A, Suurd DPD, van Rooij R, *et al.* SUV normalisation and reference tissue selection for [(1)(8)F]mFBG PET-CT in paediatric and adult patients. *Eur J Nucl Med Mol Imaging*. 2025;52(10):3773-3780.

doi: 10.1007/s00259-025-07242-x

20. Keramida G, Peters AM. The appropriate whole body metric for calculating standardised uptake value and the influence of sex. *Nucl Med Commun*. 2019;40(1):3-7.

doi: 10.1097/MNM.0000000000000935

21. Boellaard R, Delgado-Bolton R, Oyen WJ, *et al.* FDG PET/CT: EANM procedure guidelines for tumour imaging: version 2.0. *Eur J Nucl Med Mol Imaging*. 2015;42(2):328-354.

doi: 10.1007/s00259-014-2961-x

22. Abd-Elkader MS, Elmaghraby SM, Abdel-Mohsen MA, *et al.* Estimation of liver standardized uptake value in F18-FDG PET/CT scanning: impact of different malignancies, blood glucose level, body weight normalization, and imaging systems. *Ann Nucl Med*. 2025;39(2):176-188.

doi: 10.1007/s12149-024-01985-7

23. Pan JJ, Mai HQ, Ng WT, *et al.* Ninth Version of the AJCC and UICC Nasopharyngeal Cancer TNM Staging Classification. *JAMA Oncol*. 2024;10(12):1627-1635.

doi: 10.1001/jamaoncol.2024.4354

24. Burger IA, Vargas HA, Beattie BJ, *et al.* How to assess background activity: introducing a histogram-based analysis as a first step for accurate one-step PET quantification. *Nucl Med Commun*. 2014;35(3):316-324.

doi: 10.1097/MNM.0000000000000045

25. Wang XY, Zhao YF, Liu Y, *et al.* Comparison of different automated lesion delineation methods for metabolic tumor volume of 18F-FDG PET/CT in patients with stage I lung adenocarcinoma. *Medicine*. 2017;96(51):e9365.

doi: 10.1097/MD.0000000000009365

26. Sher A, Lacoeuille F, Fosse P, *et al.* For avid glucose tumors, the SUV peak is the most reliable parameter for [(18)F] FDG-PET/CT quantification, regardless of acquisition time. *EJNMMI Res*. 2016;6(1):21.

doi: 10.1186/s13550-016-0177-8

27. Chen K, Cypess A, Laughlin M, *et al.* Brown Adipose Reporting Criteria in Imaging STudies (BARCIST 1.0): Recommendations for Standardized FDG-PET/CT Experiments in Humans. *Cell Metabolism*. 2016;24(2):210-222.

28. Wahl RL, Jacene H, Kasamon Y, *et al.* From RECIST to PERCIST: Evolving Considerations for PET response criteria

in solid tumors. *J Nucl Med*. 2009;50(Suppl 1):122S-150S.

doi: 10.2967/jnumed.108.057307

29. Kong FF, Pan GS, Ni MS, *et al.* Prognostic value of lymph node-to-primary tumor ratio of PET standardized uptake value for nasopharyngeal carcinoma: a recursive partitioning risk stratification analysis. *Ther Adv Med Oncol*. 2024;16:17588359241233235.

doi: 10.1177/17588359241233235

30. Li XB, Gu JD, Zhou QH. Review of aerobic glycolysis and its key enzymes - new targets for lung cancer therapy. *Thorac Cancer*. 2015;6(1):17-24.

doi: 10.1111/1759-7714.12148

31. Wu Z, Wu J, Zhao Q, *et al.* Emerging roles of aerobic glycolysis in breast cancer. *Clin Transl Oncol*. 2020;22(5):631-646.

doi: 10.1007/s12094-019-02187-8

32. Xiao BB, Lin DF, Sun XS, *et al.* Nomogram for the prediction of primary distant metastasis of nasopharyngeal carcinoma to guide individualized application of FDG PET/CT. *Eur J Nucl Med Mol Imaging*. 2021;48(8):2586-2598.

doi: 10.1007/s00259-020-05128-8

33. Hua HL, Deng YQ, Li S, *et al.* Deep Learning for Predicting Distant Metastasis in Patients with Nasopharyngeal Carcinoma Based on Pre-Radiotherapy Magnetic Resonance Imaging. *Comb Chem High Throughput Screen*. 2023;26(7):1351-1363.

doi: 10.2174/1386207325666220919091210

34. Lou Y, Chen D, Lin Z, *et al.* The prognostic value of the ratio of standard uptake value of lymph node to primary tumor before treatment of locally advanced nasopharyngeal carcinoma. *Eur Arch Otorhinolaryngol*. 2023;280(1):347-356.

doi: 10.1007/s00405-022-07562-w

35. Pellegrino S, Fonti R, Torbati AHM, *et al.* Heterogeneity of glycolytic phenotype determined by ^{18}F-FDG PET/CT using coefficient of variation in patients with advanced non-small cell lung cancer. *Diagnostics*. 2023;13(14):2448.

doi: 10.3390/diagnostics13142448

36. Cruz C, Barba I. Lactic acid in tumour biology. *Metabolites*. 2026;16(1):75.

doi: 10.3390/metabo16010075

37. Lee JW, Ahn H, Yoo ID, *et al.* Relationship of FDG PET/CT imaging features with tumor immune microenvironment and prognosis in colorectal cancer. *Cancer Imaging*. 2024;24(1):53.

doi: 10.1186/s40644-024-00698-4

38. Claeys J, Mertens K, D'Asseler Y, *et al.* Normoglycemic plasma glucose levels affect F-18 FDG uptake in the brain. *Ann Nucl Med*. 2010;24(6):501-5.

doi: 10.1007/s12149-010-0359-9

39. Turcotte E, Leblanc M, Carpentier A, *et al.* Optimization of whole-body positron emission tomography imaging by using delayed 2-deoxy-2-[F-18]fluoro-D: -glucose Injection following I.V. Insulin in diabetic patients. *Mol Imaging Biol*. 2006;8(6):348-354.

doi: 10.1007/s11307-006-0064-1